Appl. Phys. B 82, 403–406 (2006)
DOI: 10.1007/s00340-005-2054-4

Applied Physics B
Lasers and Optics

Y.F. CHEN ✉
L.Y. TSAI

Comparison between shared and coupled resonators for passively Q-switched $Nd:GdVO_4$ intracavity optical parametric oscillators

Department of Electrophysics, National Chiao Tung University, 1001 TA Hsueh Road, Hsinchu, Taiwan

Received: 19 July 2005/Revised version: 8 September 2005
Published online: 30 November 2005 •

ABSTRACT Comparison between the shared and coupled resonators for the intracavity optical parametric oscillators pumped by passively Q-switched $Nd:GdVO_4$ lasers is experimentally made. The shared and coupled resonators are found to be complementary in the performances of the pulse repetition rate, pulse duration and pulse energy. It is also found that the output signal pulses of the shared cavity explicitly display the mode-locking phenomenon. On the whole, the amplitude stability of the shared cavity configuration is substantially superior to that of the coupled cavity configuration.

PACS 42.60.Gd; 42.65.Yj; 42.55.Xi

1 Introduction

Nanosecond pulsed lasers at the eye-safe wavelength region (1.5–1.6 μm) are indispensable to applications such as telemetry and range finders. One promising approach for high-peak-power eye-safe laser sources is based on intracavity optical parametric oscillators (OPOs) [1–4]. The advent of high-damage-threshold nonlinear crystals and diode-pumped Nd-doped lasers have lead to a renaissance of interest in intracavity OPOs [2–4]. Recently, we demonstrated a compact efficient eye-safe OPO pumped by a diode-pumped passively Q-switched $Nd:YVO_4$ laser to produce peak powers at 1573 nm higher than 1 kW [5]. Compared with $Nd:YVO_4$ lasers, all the experimental results to date have revealed that $Nd:GdVO_4$ crystals may be potentially more competent than $Nd:YVO_4$ crystals in diode-pumped solid-state lasers due to its high absorption coefficient and large thermal conductivity [6–14]. More recently, we demonstrated a diode-pumped passively Q-switched $Nd:GdVO_4$/KTP/Cr^{4+}:YAG intracavity OPO with the output peak powers higher than 10 kW [15].

So far, to our knowledge, all resonator configurations for intracavity OPOs pumped by diode-pumped Q-switched Nd-doped lasers [2–4, 15–17] are based on the coupled cavity in which there are separate resonators for the signal and pump optical fields, as shown in Fig. 1a. Experimental results revealed that the amplitude stability of the signal outputs for the coupled cavity configuration is severely dependent on the cavity alignment because the resonator lengths and the longitudinal-mode spacing are different for the pump and signal beams. The investigations of the intracavity Raman oscillation [18] revealed that the shared cavity configuration in which the pump and Stokes beams share the same resonator is more reliable than the coupled cavity configuration. Even though the concept of the shared cavity has been proposed for nearly 30 years, this configuration is never applied to the diode-pumped Nd-doped lasers with intracavity OPOs.

In this work we make a thorough comparison between the shared and coupled resonators for the output performances of the intracavity OPOs pumped by diode-pumped passively Q-switched $Nd:GdVO_4$/Cr^{4+}:YAG lasers with the nearly hemispherical cavities. At an incident pump power of

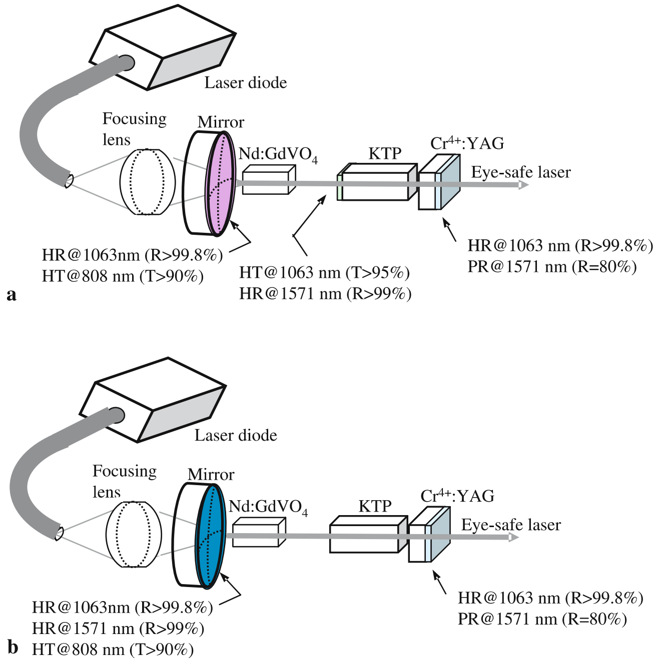

FIGURE 1 Schematix of the intracavity OPOs pumped by diode-pumped passively Q-switched $Nd:GdVO_4$/Cr^{4+}:YAG lasers, (**a**) the coupled cavity, (**b**) the shared cavity

✉ Fax: (886) 35-725230, E-mail: yfchen@cc.nctu.edu.tw

15 W, the coupled cavity produces an average signal powers of 1.2 W with a pulse repetition rate of 46 kHz and a pulse width of 0.6 ∼ 0.7 ns, whereas the shared cavity generates an average signal powers of 0.94 W with a pulse repetition rate of 21 kHz and a pulse width of 2.2 ∼ 2.5 ns. The experimental results indicate that the shared and coupled resonators are complementary in the performances. Even so, the amplitude stability of the shared cavity configuration is substantially superior to that of the coupled cavity configuration.

2 Experimental setup

Figure 1a represents the coupled resonator configuration used in our previous work, whereas Fig. 1b displays the new configuration that is a shared resonator. Here the performance of passive Q-switching for both configurations was enhanced by use of the nearly hemispherical resonators to reach second threshold criterion [19–21]. Moreover, we employed a coated Cr^{4+}:YAG crystal to simultaneously serve as a saturable absorber as well as an output coupler. The Cr^{4+}:YAG crystal has a thickness of 3 mm with 80% initial transmission at 1063 nm. One side of the Cr^{4+}:YAG crystal was coated so that it was nominally highly reflecting at 1063 nm ($R > 99.8\%$) and partially reflecting at 1571 nm ($Rs = 80\%$). The remaining side was coated for antireflection at 1063 and 1571 nm. The active medium was an a-cut 0.25 at. % Nd^{3+}, 8-mm-long Nd:$GdVO_4$ crystal. Both sides of the laser crystal were coated for antireflection at 1063 nm ($R < 0.2\%$). The reflectivity of the Nd:$GdVO_4$ crystal surface at 1571 nm was found to be approximately 3%. A Nd:$GdVO_4$ crystal with low doping concentration was used to avoid the thermally induced fracture [22]. The 20-mm-long KTP crystal was used in type II noncritical phase-matching configuration along the x-axis ($\theta = 90°$ and $\phi = 0°$) to have both a maximum effective nonlinear coefficient and no walk-off between the pump, signal, and idler beams. All crystals were wrapped with indium foil and mounted in water-cooled copper blocks. The water temperature was maintained at 25 °C. The pump source was a 16-W 808-nm fiber-coupled laser diode with a core diameter of 800 µm and a numerical aperture of 0.2. Focusing lens with 12.5 mm focal length and 92% coupling efficiency was used to re-image the pump beam into the laser crystal. The pump spot radius was around 350 µm. The input mirror was a 50 mm radius-of-curvature concave mirror and the overall cavity length for the Nd:$GdVO_4$ laser was approximately 60 mm.

For the coupled cavity configuration, as shown in Fig. 1a, the OPO cavity was formed by a coated KTP crystal and a coated Cr^{4+}:YAG crystal and the OPO cavity length was about 25 mm. One side of the KTP crystal was coated to have high reflection at the signal wavelength of 1571 nm ($R > 99.8\%$) and high transmission at the pump wavelength of 1063 nm ($T > 95\%$). The other side of the KTP crystal was coated for antireflection at 1571 nm and 1063 nm. The input mirror of the coupled resonator had antireflection coating at the diode wavelength on the entrance face ($R < 0.2\%$) and high-reflection coating at lasing wavelength ($R > 99.8\%$) and high-transmission coating at the diode wavelength on the other surface ($T > 95\%$).

For the shared resonator configuration, as shown in Fig. 1b, the OPO cavity entirely overlapped with the pump laser cavity. To setup the shared cavity, the input mirror had antireflection coating at the pump wavelength (∼ 808 nm) on the entrance face ($R < 0.2\%$) and high-reflection coating at 1063 nm and 1571 nm ($R > 99.8\%$) and high-transmission coating at the pump wavelength on the other surface ($T > 90\%$). On the other hand, the both sides of the KTP crystal for the shared cavity were coated for antireflection at 1571 nm and 1063 nm.

3 Experimental results

Figure 2 shows the average output powers at 1571 nm with respect to the incident pump powers for two types of intracavity OPOs. It was found that the threshold pump powers for both cavities were nearly the same to be 3.7 W. At an incident pump power of 15 W, the average output powers for the coupled and shared cavities were 1.2 W and 0.94 W, respectively. The conversion efficiencies from the laser diode input powers to the OPO signal output powers were 8.0% and 6.3%, respectively.

The pulse temporal behavior at 1063 nm and 1571 nm was recorded by a LeCroy digital oscilloscope (Wavepro 7100; 10 Gsamples/sec; 1 GHz bandwidth) with a fast InGaAs photodiode. Figure 3 depicts the pulse repetition rates at 1571 nm versus the incident pump powers for two types of intracavity OPOs. For the coupled cavity, it was found that the pulse repetition rates initially increased with the pump powers, and began to saturate at 40 ∼ 46 kHz for the incident pump powers greater than 9 W. On the other hand, the pulse repetition rates of the shared cavity initially increased with the pump powers, and began to saturate at 20 ∼ 24 kHz for the incident pump powers greater than 6 W. From Figs. 2 and 3, it can be seen that both intracavity OPOs have very comparable performances at the pump pow-

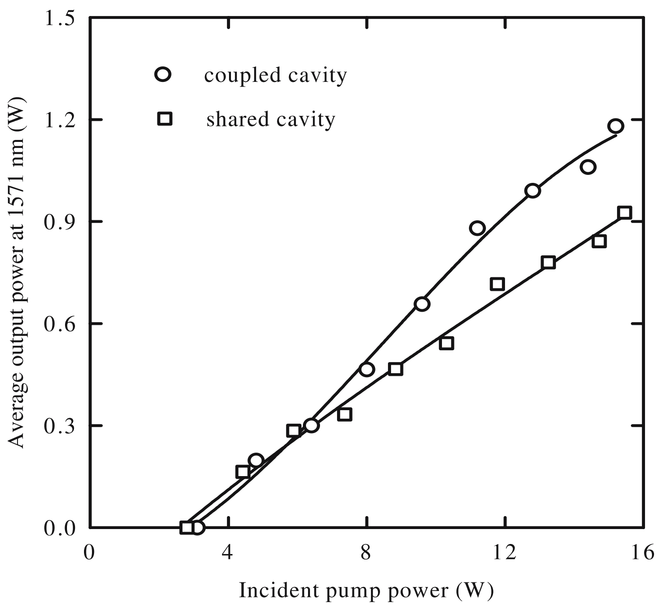

FIGURE 2 Average output powers at 1571 nm with respect to the incident pump powers for two types of intracavity OPO's

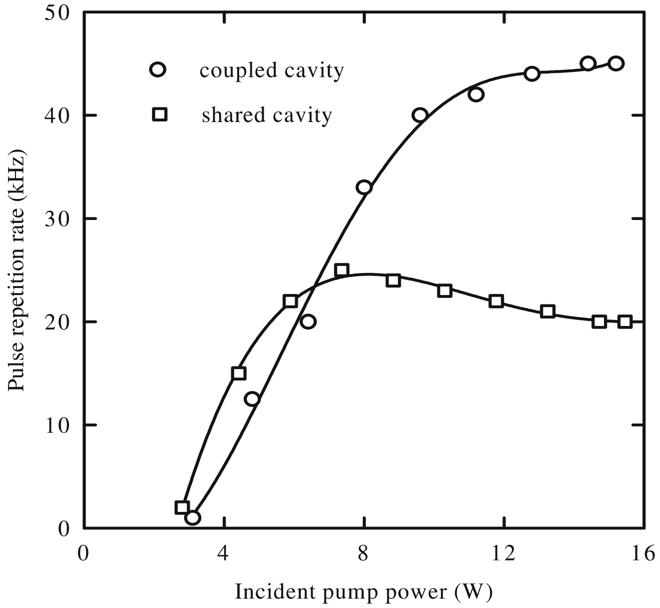

FIGURE 3 Pulse repetition rates at 1571 nm versus the incident pump powers for two types of intracavity OPOs

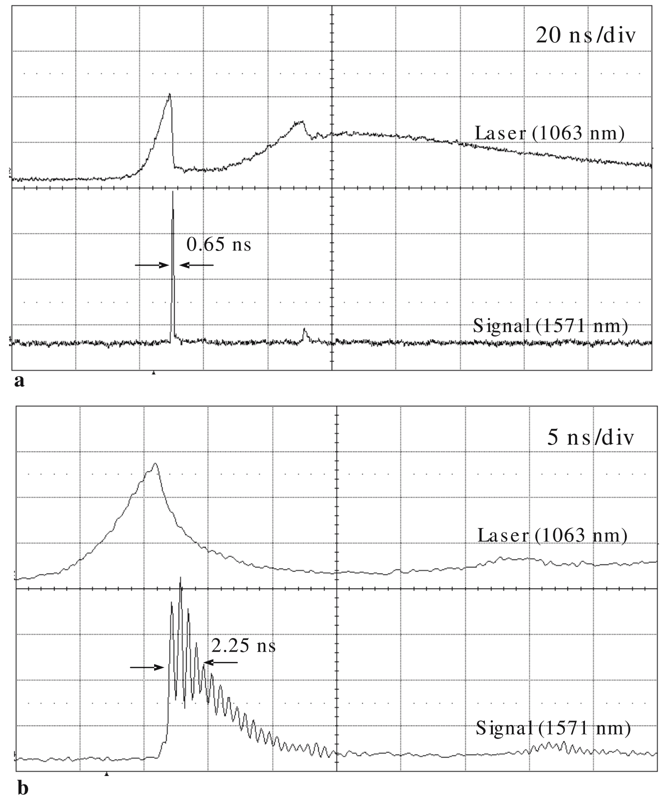

FIGURE 5 Typical temporal shapes for the laser and signal pulses, (**a**) the coupled cavity, (**b**) the shared cavity

ers less than 7 W, whereas the performance difference at the pump powers higher than 9 W is mainly subject to the pulse repetition rate and weakly dependent on the average output power.

Figure 4 plots the pulse energies at 1571 nm versus the incident pump powers for two types of intracavity OPOs. It is seen that the difference between the pulse energies for two intracavity OPOs is not significant for the pump powers less than 7 W. However, the pulse energies of the shared cavity are considerably higher than those of the coupled cavity for the pump power higher than 10 W because its lower pulse repetition rates, as shown in Fig. 3. At an incident pump power of 15 W, the maximum pulse energies were 26 μJ and 46 μJ for the coupled and shared resonators, respectively.

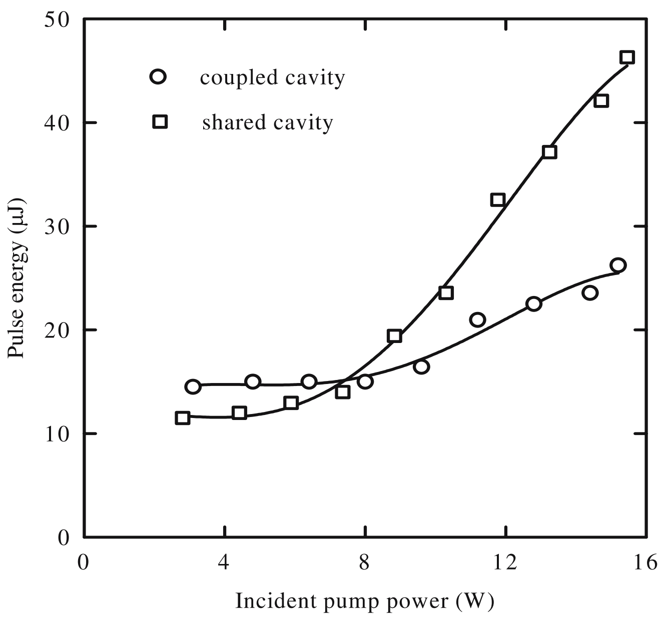

FIGURE 4 Pulse energies at 1571 nm versus the incident pump powers for two types of intracavity OPOs

Figure 5a and b are the typical temporal shapes of the laser and signal pulses for the coupled and shared cavities, respectively. The pulse durations of the signal outputs were as short as $0.6 \sim 0.7$ ns for the coupled cavity. In addition, a second signal pulse may be occasionally produced for the pump power higher than 10 W. On the other hand, the signal outputs of the shared cavity were found to display the mode-locking phenomenon; the pulse envelopes have temporal durations of $2.2 \sim 2.5$ ns. The repetition rate of the mode-locked pulses inside the Q-switched pulses is approximately to be 1.8 GHz. Even though the Q-switched pulse duration of the shared cavity is $3 \sim 4$ times longer than the pulse duration of the coupled cavity, its higher pulse energy and mode-locking phenomenon result in its maximum peak power up to 20 kW, comparable to that of the coupled cavity. We speculate that the fluctuation mechanism [23] is responsible for generating mode-locked pulses. According to the fluctuation mechanism [23], the signal wave consists of a chaotic collection of ultrashort peaks in the build-up stage due to the interference of a great number of modes having a random phase distribution, whereas the most intensive fluctuation peaks are amplified faster than all weaker ones in the nonlinear stage. We also conjecture that the high reflectivity at 1064 nm leads to the mode-locking phenomenon for the fundamental wave to be insignificant. For the coupled cavity, the OPO and laser resonators have different longitudinal mode spacings in the coupled cavity; mostly only one longitudinal laser mode is utilized to pump the OPO and only one signal longitudinal mode builds up.

The mode-locking phenomenon reveals that all the longitudinal laser modes in the shared cavity are simultaneously excited to reach OPO threshold. As a consequence, the OPO performance of the shared cavity basically depends on the total laser power of all longitudinal modes not on the explicit distribution of the laser power among the longitudinal modes. On the other hand, the small perturbations in the stable resonators usually lead to considerable variations in the power distribution among the longitudinal modes and do not significantly affect the total laser power. Therefore, the amplitude stability of the shared cavity configuration is substantially superior to that of the coupled cavity configuration. The fluctuations of the average output powers over hours-long operation without any cavity realignment are found to be $\pm 3.5\%$ and $\pm 10\%$ for the shared and coupled cavities, respectively. Our experimental results are essentially consistent with the findings in the investigations of the intracavity Raman oscillator [18].

4 Summary

In summary, we employed the diode-pumped passively Q-switched Nd:$GdVO_4$ lasers to pump the intracavity OPOs and made a complete comparison between the shared and coupled resonators for the output performances. It was found that the performances of the shared and coupled resonators are complementary in many respects. The shared cavity, for example, produces the Q-switched pulse durations $3 \sim 4$ times longer than the coupled cavity does. However, the maximum peak power of the shared cavity is comparable to that of the coupled cavity because of its larger pulse energy and mode-locking phenomenon. Nevertheless, from a practical device viewpoint, the shared cavity configuration provides better amplitude stability for the signal outputs.

REFERENCES

1 J. Falk, J.M. Yarborough, E.O. Ammann, IEEE J. Quantum Electron. **QE-7**, 359 (1971)
2 R.S. Conroy, C.F. Rae, G.J. Friel, M.H. Dunn, B.D. Sinclair, J.M. Ley, Opt. Lett. **23**, 1348 (1998)
3 A.R. Geiger, H. Hemmati, W.H. Farr, N.S. Prasad, Opt. Lett. **21**, 201 (1996)
4 O.B. Jensen, T. Skettrup, O.B. Petersen, M.B. Larsen, J. Opt. A: Pure Appl. Opt. **4**, 190 (2002)
5 Y.F. Chen, S.W. Chen, Y.C. Chen, Y.P. Lan, S.W. Tsai, Appl. Phys. B **77**, 493 (2003)
6 A.I. Zagumennyi, V.G. Ostroumov, I.A. Shcherbarkov, T. Jensen, J.P. Meyn, G. Huber, Sov. J. Quantum Electron. **22**, 1071 (1992)
7 T. Jensen, V.G. Ostroumov, J.P. Meyn, G. Huber, A.I. Zagumennyi, I.A. Shcherbarkov, Appl. Phys. B **58**, 373 (1994)
8 V. Lupei, N. Pavel, Y. Sato, T. Taira, Opt. Lett. **28**, 2366 (2003)
9 T. Ogawa, Y. Urata, S. Wada, K. Onodera, H. Machida, H. Sagae, M. Higuchi, K. Kodaira, Opt. Lett. **28**, 2333 (2003)
10 J. Liu, B. Ozygus, S. Yang, J. Erhard, U. Seelig, A. Ding, H. Weber, X. Meng, L. Zhu, L. Qin, C. Du, X. Xu, Z. Shao, J. Opt. Soc. Am. B **20**, 652 (2003)
11 C. P. Wyss, W. Luthy, H.P. Weber, V.I. Vlasov, Y.D. Zavartsev, P.A. Studenikin, A.I. Zagumennyi, I.A. Shcherbakov, Appl. Phys. B **68**, 659 (1999)
12 D.Y. Shen, H.R. Yang, J.G. Liu, S.C. Tam, Y.L. Lam, W.J. Xie, J.H. Gu, K. Ueda, Appl. Phys. B **72**, 263 (2001)
13 C. Du, L. Qin, X. Meng, G. Xu, Z. Wang, X. Xu, L. Zhu, B. Xu, Z. Shao, Opt. Commun. **212**, 177 (2002)
14 C. Du, L. Qin, H. Zhang, X. Meng, G. Xu, Z. Wang, X. Xu, L. Zhu, B. Xu, J. Wang, Z. Shao, Jpn. J. Appl. Phys. **42**, 5063 (2003)
15 Y.F. Chen, S.W. Chen, L.Y. Tsai, Y.C. Chen, C.H. Chien, Appl. Phys. B **79**, 823 (2004)
16 A. Agnesi, S. Dell'Acqua, G. Reali, Appl. Phys. B **70**, 751 (2000)
17 W. Zendzian, J.K. Jabczyñski, J. Kwiatkowski, Appl. Phys. B **76**, 355 (2003)
18 E.O. Ammann, Appl. Phys. Lett. **32**, 52 (1978)
19 A.E. Siegman, *Laser*, (University Science, Mill Valley, Calif. 1986), p. 1024 and p. 1012.
20 Y.F. Chen, S.W. Tsai, IEEE J. Quantum Electron. **QE-37**, 586 (2001)
21 Y.F. Chen, Y.P. Lan, H.L. Chang, IEEE J. Quantum Electron. **QE-37**, 462 (2001)
22 Y.F. Chen, IEEE J. Quantum Electron. **QE-35**, 234 (1999)
23 J.A. Fleck, Phys. Rev. B **1**, 84 (1970)